Polymer Bulletin 32, 249–256 (1994)

Polymer Bulletin

Synthesis and mesomorphic behavior of poly[(2*S*, 3*S*)-(+)-2-chloro-3-methylpentyl 4'-(ω-vinyloxyalkyloxy)biphenyl-4-carboxylate]s with ethyl and propyl alkyl groups

V. Percec* and Q. Zheng

Department of Macromolecular Science, Case Western Reserve University, Cleveland, OH 44106, USA

Summary

The synthesis and cationic polymerization of (2S, 3S)-(+)-2-chloro-3-methylpentyl 4'-(2-vinyloxyethyloxy)biphenyl-4-carboxylate (**15-2**) and (2S, 3S)-(+)-2-chloro-3-methylpentyl 4'-(3-vinyloxypropyloxy)biphenyl-4-carboxylate (**15-3**) are described. The mesomorphic behavior of the resulting polymers is discussed as a function of the molecular weight and spacer length. Based on the second and subsequent heating and cooling scans, poly(**15-2**)s exhibit an enantiotropic S_X (unidentified smectic) phase. Poly(**15-2**) with DP=4 is only crystalline. Poly(**15-3**)s show an enantiotropic cholesteric phase and an inverse monotropic S_X phase.

Introduction

Previous publications from our laboratory have reported the synthesis and cationic polymerization of chiral mesogenic vinyl ether monomers based on (2S, 3S)-(+)-2-chloro-3-methylpentyl 4'-(ω-vinyloxyalkyloxy)biphenyl-4-carboxylate (**15-n**) with undecanyl, octyl and hexyl groups as spacers (n=11, 8, and 6)[1,2]. The polymerizations of **15-n** were performed with the $CF_3SO_3H/(CH_3)_2S$ initiating system at 0°C in CH_2Cl_2 to give polymers with well controlled molecular weight and narrow polydispersities[3]. The phase behavior of the resulting polymers was discussed as a function of the molecular weight and spacer length. Poly(**15-11**)s and poly(**15-8**)s exhibit enantiotropic S_A, S_C^* and S_X (unidentified smectic) phases, while poly(**15-6**)s enantiotropic S_C^* and S_X phases. Copolymerization was used to suppress crystalline and S_X phases present in the homopolymers and generate a S_C^* phase at room temperature[1,4,5]. In order to provide a complete understanding of the influence of the molecular weight and spacer length on the phase behavior of this series of polymers, the homologous monomers and polymers with shorter spacers were synthesized and characterized.

The goal of this paper is to describe the synthesis and cationic polymerization of (2S, 3S)-(+)-2-chloro-3-methylpentyl 4'-(2-vinyloxyethyloxy)biphenyl-4-carboxylate (**15-2**) and (2S, 3S)-(+)-2-chloro-3-methylpentyl 4'-(3-vinyloxypropyloxy)biphenyl-4-carboxylate (**15-3**). The phase behavior of the resulting polymers will be discussed as a function of molecular weight and spacer length.

Experimental

Materials

2-Chloroethyl vinyl ether (99%, Aldrich), n-butyl vinyl ether (98%, Aldrich), 3-chloropropyl-1-ol (99%, Aldrich), 1,10-phenanthroline (anhydrous, 99%, Lancaster) and palladium (II) diacetate (from Lancaster) were used as received. CH_2Cl_2 (from Fisher) was first washed with concentrated H_2SO_4 several times until the acid layer remained colorless, then washed with water, dried over anhydrous $MgSO_4$, refluxed over CaH_2 and

*Corresponding author

freshly distilled under argon before each use. $(CH_3)_2S$ (anhydrous, 99%, from Aldrich) was refluxed and then distilled over sodium metal under nitrogen. CF_3SO_3H (98%, from Aldrich) was distilled under vacuum. Other reagents and compounds were described previously[1,2,5].

Techniques

^{1}H-NMR (200 MHz) spectra were recorded on a Varian XL-200 spectrometer. Infrared (IR) spectra were recorded on a Perkin-Elmer 1320 infrared spectrophotometer. Relative molecular weights of polymers were measured against polystyrene standards by gel permeation chromatography (GPC) with a Perkin-Elmer Series 10 LC instrument equipped with LC-100 column oven and a Nelson Analytical 900 series integrator data station. A set of two Perkin-Elmer PL gel columns of $5x10^2$ and 10^4 Å with THF as solvent (1ml/min) were used. The measurements were made at 40°C using the UV detector. High pressure liquid chromatography (HPLC) experiments were performed with the same instrument. Phase transition temperatures were determined by a Perkin-Elmer DSC-7 differential scanning calorimeter equipped with TAC 7/DX thermal analysis controller. In all cases, heating and cooling rates were 20°C/min. Glass transition temperatures (T_g) were read at the middle of the change in the heat capacity. A Carl-Zeiss optical polarized microscope equipped with a Mettler FP 82 hot stage and a Mettler FP 80 central processor was used to observe the thermal transitions and to verify the anisotropic textures.

Synthesis of (2S, 3S)-(+)-2-chloro-3-methylpentyl 4'-(2-vinyloxyethyloxy)biphenyl-4-carboxylate (**15-2**) and (2S, 3S)-(+)-2-chloro-3-methylpentyl 4'-(3-vinyloxypropyloxy) biphenyl-4-carboxylate (**15-3**)

The synthetic procedures for **15-2** and **15-3** are presented in Scheme 1, where the number assignment for compounds starts with **10-n** in order to maintain the same nomenclature for the monomers of this series as in the previous publications. The synthesis of **12**, **14** and of other compounds was described in the previous publications[1,2,5].

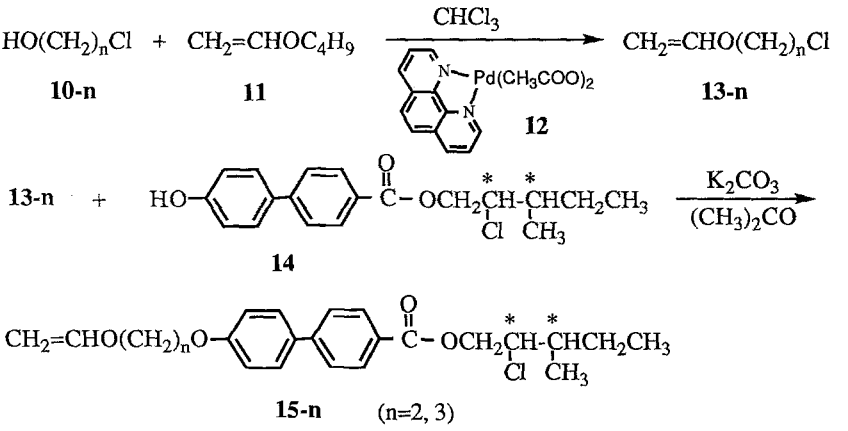

Scheme 1. Synthesis of (2S, 3S)-(+)-2-chloro-3-methyl-pentyl 4'-(2-vinyloxyethyloxy) biphenyl-4-carboxylate (**15-2**) and (2S, 3S)-(+)-2-chloro-3- methylpentyl 4'-(3-vinyloxypropyloxy) biphenyl-4-carboxylate (**15-3**).

(2S, 3S)-(+)-2-Chloro-3-methylpentyl 4'-(2-vinyloxyethyloxy)biphenyl-4-carboxylate (**15-2**)

2-Chloroethyl vinyl ether (**13-2**) (1.6 g, 15.0mmol) was added to a mixture of **14** (5.0 g, 15.0mmol), K_2CO_3 (6.2g, 45.0mmol), KI (5.0g, 30.0mmol) and 90ml of acetone and the reaction was stirred at 60°C for 30 min. After refluxing at 65°C for 8 h, the reaction mixture was poured into 150ml of H_2O. The crude product was extracted with diethyl ether (4x60ml), and the combined ether extract was washed with H_2O and dried over anhydrous $MgSO_4$. After the ether was distilled on a rotary evaporator, the remaining product was purified by column chromatography (silica gel, CH_2Cl_2/C_6H_{14}=2/1 as eluent), followed by recrystallization from methanol to produce monomer **15-2** as white crystals (2.8 g, 46%). Purity: >99% (HPLC). mp: 56.2°C. ^{1}H-NMR ($CDCl_3$, TMS, δ, ppm): 0.97 (t, J=7.6Hz, 3H, C<u>H</u>$_3$CH$_2$-), 1.10 (d, J=6.5Hz, 3H, C<u>H</u>$_3$CH(CH$_2$CH$_3$)-), 1.38-1.62 (m, 2H, CH$_3$C<u>H</u>$_2$-), 1.93 (m, 1H, CH$_3$CH$_2$C<u>H</u>(CH$_3$)-), 4.08 (m, 3H, =CH-OC<u>H</u>$_2$- and =C<u>H</u>$_2$ trans), 4.15-4.25 (m, 3H, -C<u>H</u>$_2$-OPh, and =C<u>H</u>$_2$ cis), 4.55 (m, 3H, -COOC<u>H</u>$_2$- and -C<u>H</u>(Cl)-), 6.50-6.61 (m, 1H, =C<u>H</u>-O-), 7.03 (d, J=8.7Hz, 2 ArH, o to -O(CH$_2$)$_2$-), 7.56 (d, J=7.9Hz, 2 ArH, m to O(CH$_2$)$_2$-), 7.65 (d, J=8.3Hz, 2 ArH, m to -COO-), 8.11 (d, J=7.4Hz, 2 ArH, o to -COO-).

3-Chloropropyl-1-vinyl ether (**13-3**)

The mixture of 3-chloropropan-1-ol (**10-3**) (3.7g, 38.7mmol), 1,10-phenanthroline palladium (II) diacetate (**12**)[5] (0.5g, 1.2mmol), 85ml of n-butyl vinyl ether (**11**) and 20ml of dry $CHCl_3$ was heated to reflux at (60°C) for 14 h. The resulting dark green suspension was filtered, and the filtrate was distilled on a rotary evaporator to remove excess n-butyl vinyl ether and $CHCl_3$. The resulting light yellow oil was purified by column chromatography (silica gel, CH_2Cl_2/C_6H_{14}=1/4 as eluent) to yield a colorless liquid (2.4g, 51%). ^{1}H-NMR ($CDCl_3$, TMS, δ, ppm): 2.03 (m, 2H, -C<u>H</u>$_2$-CH$_2$Cl), 3.84 (m, 4H, =CHOC<u>H</u>$_2$- and C<u>H</u>$_2$-Cl), 3.99 (d, J=6.8Hz, 1H, =C<u>H</u>$_2$, trans), 4.16 (d, J=14.1Hz, 1H, =C<u>H</u>$_2$, cis), 6.40-9.53 (m, 1H, =C<u>H</u>-O-).

(2S, 3S)-(+)-2-Chloro-3-methylpentyl 4'-(3-vinyloxypropyloxy)biphenyl-4-carboxylate (**15-3**)

15-3 was synthesized by the same procedure as that used for **15-2**. Starting from **13-3** (1.2g, 10.3mmol) and **14** (3.4g, 10.3mmol), **15-3** was obtained as white crystals (2.5g, 58%). Purity: >99% (HPLC). mp: 55.3°C. ^{1}H-NMR ($CDCl_3$, TMS, δ, ppm): 0.97 (t, J=7.0Hz, 3H, C<u>H</u>$_3$CH$_2$-), 1.09 (d, J=7.1Hz, 3H, C<u>H</u>$_3$CH(CH$_2$CH$_3$)-), 1.34-1.63 (m, 2H, CH$_3$C<u>H</u>$_2$-), 1.93 (m, 1H, CH$_3$CH$_2$C<u>H</u>(CH$_3$)-), 2.17 (m, 2H, -OCH$_2$C<u>H</u>$_2$CH$_2$-), 3.92 (t, J=6.4Hz, 2H, =CH-OC<u>H</u>$_2$-), 4.02 (d, J=7.2Hz, =C<u>H</u>$_2$ trans), 4.14-4.22 (m, 3H, -C<u>H</u>$_2$-OPh, =C<u>H</u>$_2$ cis), 4.55 (m, 3H, -COOC<u>H</u>$_2$- and -C<u>H</u>(Cl)-), 6.43-6.54 (m, 1H, =C<u>H</u>-O-), 7.00 (d, J=8.6Hz, 2 ArH, o to -O(CH$_2$)$_3$-), 7.57 (d, J=8.3Hz, 2 ArH, m to O(CH$_2$)$_3$-), 7.63 (d, J=8.4Hz, 2 ArH, m to -COO-), 8.11 (d, J=7.1Hz, 2 ArH, o to -COO-).

Cationic Polymerizations

Polymerizations were carried out in a three-neck round bottom flask equipped with Teflon stopcock and rubber septum under argon atmosphere at 0°C for 1 h. All glassware was dried overnight at 140°C. The monomer was further dried under vacuum overnight in the polymerization flask. After the flask was filled with argon, freshly distilled dry CH_2Cl_2 was added through a syringe and the solution was cooled to 0°C. Freshly distilled $(CH_3)_2S$ and CF_3SO_3H were then added consecutively via a syringe. The monomer concentration was about 0.2M and the $(CH_3)_2S$ concentration was 10 times larger than that of the CF_3SO_3H. The polymer molecular weight was controlled by the monomer/initiator ($[M]_o/[I]_o$) ratio. After quenching the polymerization with ammoniacal

Table 1. Cationic polymerization of **15-2** (temperature: 0°C; solvent: CH_2Cl_2; $[M]_0$=0.2; $[(CH_3)_2S]_0/[I]_0$=10; time: 1h) and characterization of the resulting poly(**15-2**). Data on the first and second lines under heating are from the first and second heating scans, respectively. (†: Over lapped peaks)

Sample No.	$[M]_0/[I]_0$	Polymer yield(%)	$Mnx10^{-3}$	Mw/Mn	DP	phase transitions (°C) and corresponding enthalpy changes (kcal/mru)	
			GPC			heating	cooling
1	5	65	1.62	1.08	4.0	K 61.1 (2.74) i g 14.0 K 63.2 (1.63) i	i 35.1 (-0.73) K 3.0 g
2	8	62	1.67	1.09	4.6	K 55.3 (2.3) i g 15.4 K 26.1 (0.08) S_X 51.6 (0.16) i	i 18.3 (-0.02) S_X 7.9 g
3	12	54	1.97	1.06	4.7	K 54.7(2.18) i g 18.4 K 29.3 (0.07) S_X 53.2 (0.35) i	i 20.5 (-0.06) S_X 10.0 g
4	16	57	2.67	1.07	6.6	K 55.6 (†) S_X' 60.0 (0.42) S_X 82.7 (1.54) i g 53.2 S_X 84.7 (1.27) i	i 61.9 (-1.34) S_X 43.0 g
5	20	70	3.35	1.08	8.3	K 56.6 (†) S_X' 63.5 (0.44) S_X 103.6 (1.37) i g 59.9 S_X 105.2 (1.22) i	i 84.8 (-0.97) S_X 51.2 g
6	25	61	3.89	1.09	10.0	K 55.4 (†) S_X' 65.0 (0.25) S_X 107.8 (1.63) i g 60.1 S_X 107.2 (1.24) i	i 88.9 (-1.04) S_X 51.3 g

Table 2. Cationic polymerization of **15-3** (temperature: 0°C; solvent: CH_2Cl_2; $[M]_0$=0.2; $[(CH_3)_2S]_0/[I]_0$=10; time: 1h) and characterization of the resulting poly(**15-3**). Data on the first and second lines under heating are from the first heating and second heating scans, respectively. (†: Over lapped peaks)

Sample No.	$[M]_0/[I]_0$	Polymer yield(%)	$Mnx10^{-3}$	Mw/Mn	DP	phase transitions (°C) and corresponding enthalpy changes (kcal/mru)	
			GPC			heating	cooling
1	5	45	2.22	1.10	5.3	g 17.8 K 53.7 (1.24) i g 9.6 S_X 22.0 (†) Ch 32.2 (0.28) i	i 24.0 (-0.10) Ch 3.0 g
2	8	57	3.33	1.08	8.0	g 27.6 K 54.0 (1.45) i g 17.8 S_X 33.5 (†) Ch 41.7 (0.18) i	i 33.5 (-0.10) Ch 12.3 g
3	12	53	3.82	1.11	9.2	g 29.4 K 47.3 (0.76) i g 19.7 S_X 34.7 (†) Ch 42.9 (0.19) i	i 33.8 (-0.10) Ch 14.7 g
4	16	51	3.94	1.08	9.4	g 31.8 K 53.9 (1.21) i g 20.0 S_X 35.6 (†) Ch 46.1 (0.14) i	i 38.7(-0.13) Ch 16.0 g
5	20	73	4.52	1.10	10.8	g 36.0 K 47.1 (0.63) i g 21.2 S_X 36.1 (†) Ch 46.0 (0.12) i	i 39.3 (-0.08) Ch 17.4 g
6	25	74	5.06	1.11	12.1	g 41.0 K 53.2 (0.62) i g 21.6 S_X 38.3 (†) Ch 45.0 (0.17) i	i 40.2 (-0.10) Ch 17.9 g

methanol, the reaction mixture was precipitated into methanol. The resulting polymers were purified by precipitation from CH_2Cl_2 solution into methanol and were collected by filtration. All polymers obtained were dried in a vacuum oven at room temperature for more than 48 h prior to characterization.

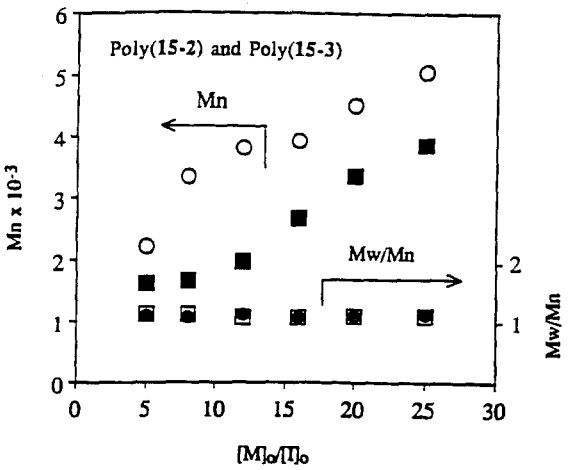

Figure 1: The dependence of number-average molecular weight (Mn) and polydispersity (Mw/Mn) of poly(**15-2**) (closed symbols) and poly(**15-3**) (open symbols) determined by GPC on the $[M]_o/[I]_o$ ratio.

Results and discussion

The polymerization results and the phase behavior of the resulting polymers [poly(**15-2**) and poly(**15-3**)] are presented in Tables 1 and 2. The polymerization yields range from 45 to 74%. The low polymerization yields are due to the polymer loss during the purification and the small scale polymerization (100mg). The relative number-average molecular weights (Mn) determined by GPC are plotted against the initial molar ratio of monomer to initiator ($[M]_o/[I]_o$) for both poly(**15-2**) and poly(**15-3**) (Figure 1). The linear relationship between Mn and $[M]_o/[I]_o$ indicates that the $[M]_o/[I]_o$ ratio provide a good control of the polymer molecular weights. Polydispersities are less than 1.12. All these features support the characteristics of a living-like polymerization. The absolute molecular weight is difficult to measure from the acetal chain end (δ=4.6ppm) of the polymer by ^{1}H-NMR due to the signal overlap with the protons of -COOC$\underline{H}_2$CH(Cl)- (δ=4.5-4.6ppm).

The phase transition temperatures and the nature of the mesophase were determined by a combination of DSC and optical polarized microscopy techniques. Figure 2a, b and c presents the DSC traces of poly(**15-2**)s obtained during the first, second heating and the first cooling scans, respectively. When determined from the first heating scan (Figure 2a) all poly(**15-2**)s show a crystalline melting peak. Poly(**15-2**)s with DP < 5 melt directly into an isotropic phase, while poly(**15-2**)s with DP > 5 melt into two unidentified smectic ($S_{X'}$ and S_X) phases. The ability towards crystallization decreases with the increase of the polymer molecular weight. During the second heating scan (Figure 2b) the kinetically controlled crystalline melting temperature was lower for poly(**15-2**)s with DP < 5, and even disappeared for poly(**15-2**)s with DP > 5. All poly(**15-2**)s with DP > 4 exhibit an enantiotropic S_X phase, while poly(**15-2**) with DP=4 is still crystalline (Figure 2b and c). The $S_{X'}$-S_X transition is also depressed due to its close proximity to the glass transition temperature (Tg). The dependence of transition temperatures on the degrees of polymerization (DP) is shown in Figure 3. The transition temperature from the S_X to the isotropic phase and the Tg of poly(**15-2**) increase with the increase of DP. However, the dependence of the transition temperature from the S_X to the isotropic phase on DP is steeper than that of Tg, leading to a wider range of the S_X phase as the molecular weight increases. The crystalline melting temperature is almost

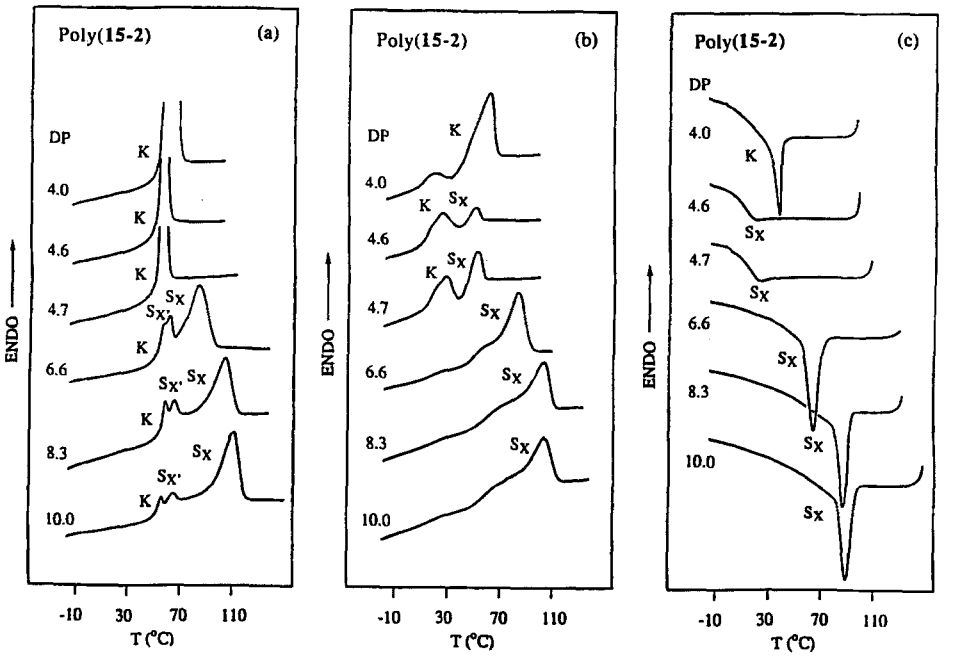

Figure 2: DSC traces of poly(15-2) with different degrees of polymerization (DP) determined by GPC. DP is printed on the top of each DSC scan: (a) first heating scan; (b) second heating scan; (c) first cooling scan.

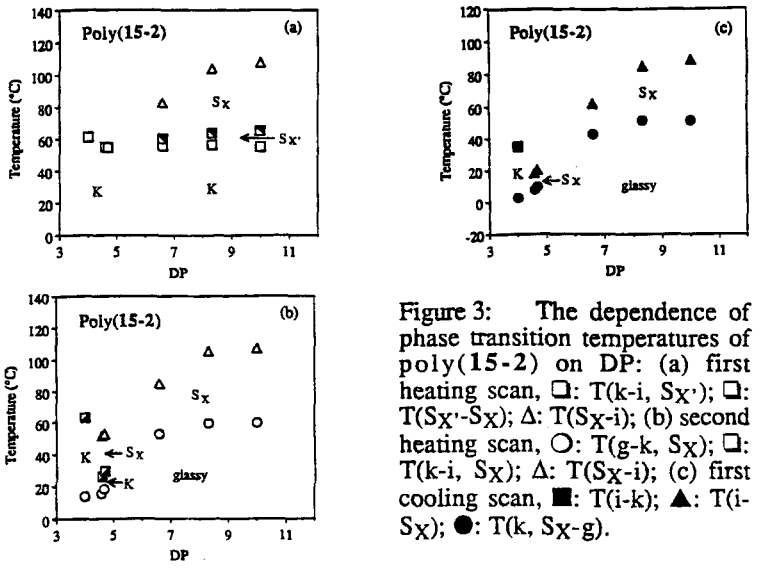

Figure 3: The dependence of phase transition temperatures of poly(15-2) on DP: (a) first heating scan, ❑: T(k-i, S_X'); ❑: T(S_X'-S_X); Δ: T(S_X-i); (b) second heating scan, ○: T(g-k, S_X); ❑: T(k-i, S_X); Δ: T(S_X-i); (c) first cooling scan, ■: T(i-k); ▲: T(i-S_X); ●: T(k, S_X-g).

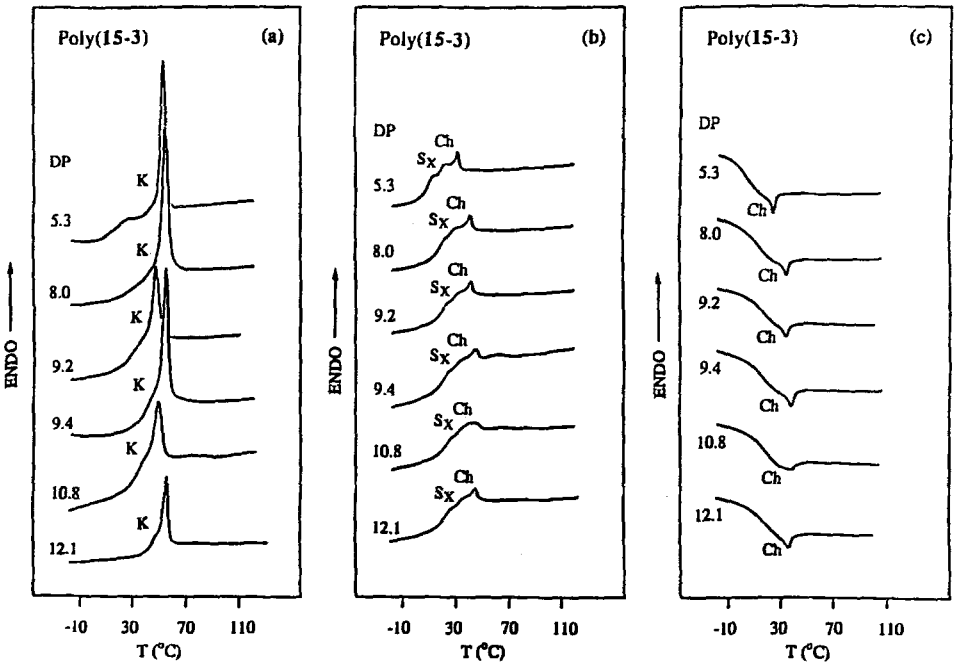

Figure 4: DSC traces of poly(15-3) with different degrees of polymerization (DP) determined by GPC. DP is printed on the top of each DSC scan: (a) first heating scan; (b) second heating scan; (c) first cooling scan.

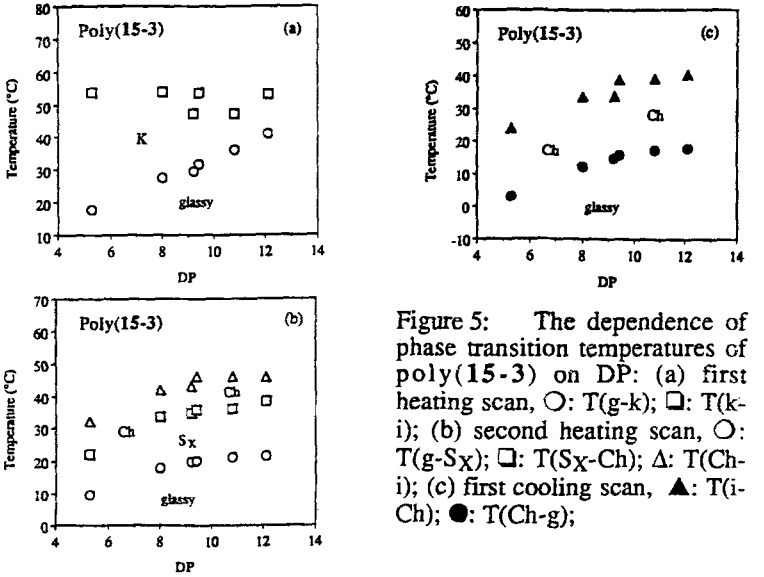

Figure 5: The dependence of phase transition temperatures of poly(15-3) on DP: (a) first heating scan, ○: T(g-k); □: T(k-i); (b) second heating scan, ○: T(g-S_X); □: T(S_X-Ch); Δ: T(Ch-i); (c) first cooling scan, ▲: T(i-Ch); ●: T(Ch-g);

independent of DP (Figure 3a), while its corresponding enthalpy change decreases (Figure 2a). However, in the second heating and the first cooling scans the crystalline phase and the higher order $S_{X'}$ (than S_X) phase do not form especially at higher molecular weights due to their close proximity to Tg and as a consequences a broader range of temperature for the S_X phase results (Figure 3b, c).

Figure 4a, b and c presents the DSC scans of poly(**15-3**)s obtained during the first, second heating and first cooling scans, respectively. Poly(**15-3**)s exhibit a crystalline phase above Tg (Figure 1a). However, during the second heating and cooling scans all poly(**15-3**)s show an enantiotropic cholesteric phase in addition to an inverse monotropic S_X phase (Figure 4b and c). The crystalline phase does not form in the second heating and cooling scans because its close proximity to Tg and its higher kinetically controlled nature than that of the liquid crystalline phases. The formation of the inverse monotropic S_X phase is due to the fact that transition temperature from the cholesteric phase to the S_X phase is too close to Tg, and therefore, is not able to form on the cooling scan. On the optical polarized microscope we observed a color change from blue to red with the increasing temperature within the cholesteric phase. The dependence of various transition temperatures on DP can be observed in Figure 5a, b and c. In this case the transition temperatures from the cholesteric phase to the S_X phase and from S_X phase to the glass state increase with the increase of DP. However, the dependence of the transition temperatures from the S_X to the cholesteric phase and from the cholesteric phase to the S_X phase on DP is similar to that of Tg. Therefore, the range of the mesophase does not change much. There is a similar situation in the case of poly{3-[(4-cyano-4'-biphenyl)oxy]propyl vinyl ether}s, where the dependence of the transition temperature from the nematic to the isotropic phase is almost identical to that of Tg[6].

The enantiotropic cholesteric phase exhibited by poly(**15-3**)s is expected based on the trends observed both in our and other laboratories related to the influence of spacer length on the nature of the mesophase[7,8]. Such a short spacer length does favor the formation of a cholesteric phase in poly(**15-3**). Because the structural unit of poly(**15-2**) is more rigid than that of poly(**15-3**), the entropy of the former system is smaller. According to some thermodynamic schemes[9,10] the isotropization temperature should be higher for the lower entropy system. Our experimental results support this prediction. The higher isotropization temperature may be also due to the higher ordered mesophase in poly(**15-2**) than that in poly(**15-3**).

Acknowledgments

Financial support from the Office of Naval Research is gratefully acknowledged.

References

1. V. Percec and Q. Zheng, *J. Mater. Chem.*, 2, 475 (1992).
2. V. Percec and Q. Zheng, *J. Mater. Chem.*, 2, 1041 (1992).
3. C. G. Chao, B. A. Feit and A. E. Webster, *Macromolecules*, 23, 1918 (1990).
4. V. Percec and C. Pugh in "*Side Chain Liquid Crystal Polymers*", C. B. McArdle Ed., Chapman and Hall, New York, 1989, p. 30.
5. V. Percec, Q. Zheng and M. Lee, *J. Mater. Chem.*, 1, 611 (1991).
6. V. Percec and M. Lee, *J. Macromol. Sci.-Chem.*, A28, 651 (1991).
7. V. Percec and D. Tomazos, *Adv. Mater.*, 4, 458 (1992).
8. V. Percec and D. Tomazos, in "*Comprehensive Polymer Science*", First Supplement, G. Allen Ed., Pergamon Press, Oxford, 1992, p. 299 and references cited therein.
9. V. Percec and A. Keller, *Macromolecules*, 23, 4347 (1990).
10. A. Keller, G. Unger and V. Percec, in "*Advances in Liquid Crystalline Polymers*", R. A. Weiss and C. K. Ober Ed., Vol. 435 in ACS Symp. Ser., Am. Chem. Soc., Washington DC, 1990.

Accepted January 31, 1994 K